PHYSICAL REVIEW B VOLUME 44, NUMBER 20 15 NOVEMBER 1991-II

Enhancement of thermal diffuse scattering by surface defects

H.-N. Yang and T.-M. Lu
Department of Physics, Rensselaer Polytechnic Institute, Troy, New York 12180-3590

(Received 26 April 1991)

The effect of surface defects on thermal diffuse scattering has been studied from the viewpoint of low-energy electron diffraction. It is concluded that thermal diffuse scattering can be enhanced significantly in the presence of surface defects, such as vacancies, adatoms, and steps. This effect basically results from surface imperfections that break up the periodic crystal ordering and lead to a deviation from the momentum-conservation law for electron-phonon scattering. This enhanced diffuse scattering has the largest effect at diffraction conditions under which the electron scatters out of phase between the top and second layers of surface atoms.

I. INTRODUCTION

Inelastic scatterings of low-energy particles (electrons, atoms, etc.) by surface excitations, including phonon scattering, have been well studied in the past two decades. For example, surface phonons are detected by using high-resolution electron-energy-loss spectroscopy,[1,2] where the electron-impact energy is typically several eV and is highly monochromatic to within a few meV. Since the phonon energy is a few tens of meV, the energy-loss peaks due to phonons can be easily identified. A similar method is thermal atom scattering,[3,4] where the primary atom energy is of order 100 meV.

In low-energy electron diffraction (LEED), phonon losses show up as a thermal diffuse intensity in the diffraction pattern. Although the energy loss due to phonon excitations is negligibly small compared with the primary electron energy (~100 eV) in LEED, the thermal diffuse scattering cannot be ignored. Thermal diffuse scattering of LEED from a perfect surface was studied a long time ago.[5-8] The phonon contribution to the diffuse LEED experimental data has also been discussed in several recent papers.[9-11]

On the other hand, LEED diffuse intensity can also come from the elastic scattering of electrons from surface defects such as steps,[12-14] vacancies,[12,15,16] and disordered adsorbates.[11,17-21] This contribution is independent of the phonon-induced inelastic scattering due to surface vibrations. In this paper, we consider the combined effects of phonons and surface defects (vacancies and steps) on the diffuse intensity.

Experimentally, it has been observed that at higher temperatures the angular profile of a LEED diffraction peak shows broad wings extending throughout the Brillouin zone.[7,8,22,23] This wing structure has been attributed to the one-phonon diffuse scatterings. Theoretically, the thermal diffuse intensity may be expressed as[6,7]

$$I_1'(\mathbf{S}_\parallel) \propto \frac{e^{-2W}\mathbf{S}^2 k_B T}{|\mathbf{S}_\parallel - \mathbf{G}_{hk}|}, \tag{1}$$

where $2W$ is the Debye-Waller factor, $\mathbf{S}$ represents the momentum transfer of the electron beam, and $\mathbf{S}_\parallel$ is its component parallel to the surface. $\mathbf{G}_{hk}$ are two-dimensional (2D) reciprocal-lattice vectors.

Equation (1) can be applied to surfaces which have negligible surface defects. For defect-free surfaces, one can present a simple picture to demonstrate the thermal diffuse scattering due to the interaction of the electrons with a vibrating surface. Figure 1 shows an atomic vibrational wave propagating along the surface with wave vector q. This vibrational wave deforms the surface elastically and forms a sinusoidal grating which has a period $d = 2\pi/q$ equal to the wavelength of the surface wave. As an electron beam is scattered by this "vibrational wave grating," a constructive interference scattering can occur under the conditions

$$S_\parallel d = 2m\pi \quad \text{where } m = 0, \pm 1, \pm 2, \ldots . \tag{2}$$

Since the wavelength d is an integer of the atomic spacing, i.e., $G_{hk} d = 2m\pi$, Eq. (2) can be generalized to

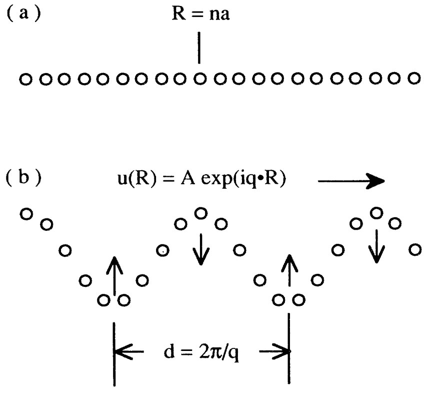

FIG. 1. (a) A 1D atomic chain which represents the surface of a rigid perfect crystal. (b) An atomic vibrational wave (transverse) with a wave vector q deforms the surface elastically and forms a sinusoidal grating of a period $d = 2\pi/q$.

$$(S_{\parallel}-G_{hk})d=2m\pi \ . \tag{2'}$$

For one-phonon scattering, $m=\pm 1$, Eq. (2′) becomes $S_{\parallel}-G_{hk}=\pm 2\pi/d=\pm q$. This, in general, can be expressed as the momentum conservation law for electron-phonon scattering,

$$\mathbf{S}_{\parallel}-\mathbf{G}_{hk}=\pm\mathbf{q}_{\parallel} \ , \tag{3}$$

where $\mathbf{q}_{\parallel}$ denotes the phonon wave vector parallel to the surface. Equation (3) reflects the origin of the thermal diffuse scattering, which is due to the vibrational wave-grating diffraction. It has been shown by Huber[6] and by Mckinney, Jones, and Webb[7] that for defect-free surfaces, the rigorous solution of the thermal diffuse intensity, Eq. (1), is a superposition of various wave-grating diffractions with different phonon wave vectors $\mathbf{q}_{\parallel}$.

However, the idea of the vibrational wave-grating diffraction can only be correct under the condition that the surface is reasonably perfect. For surfaces having substantial defects, Eq. (3) may not exist. Under this circumstance, a necessary modification is required for the conventional one-phonon scattering intensity, Eq. (1), because the thermal diffuse intensity can be significantly differed from that of a defect-free surface.

Figure 2 shows an example of a vibrational wave propagating in a stepped surface. As an electron beam is diffracted from the stepped surface of a rigid crystal, there is an extra phase difference $\Delta\phi=S_{\perp}t$, between the electrons scattered from neighboring terraces which are separated by a single atomic step. Here $S_{\perp}$ represents the momentum transfer perpendicular to the surface and t is the single-atomic-step height. Similar to $\Delta\phi$ also exists as an electron beam is scattered by the vibrational wave which propagates in a surface containing vacancies or adatoms. This extra phase difference $\Delta\phi$ must break up the diffraction grating condition, Eq. (2′), except at $\Delta\phi=S_{\perp}t=2m\pi$ (in-phase conditions). In other words, the defected surface can destroy the periodicity of the vibrational wave grating, so that the diffraction law, Eq. (3), no longer holds. This can cause a significant change in the thermal diffuse intensity.

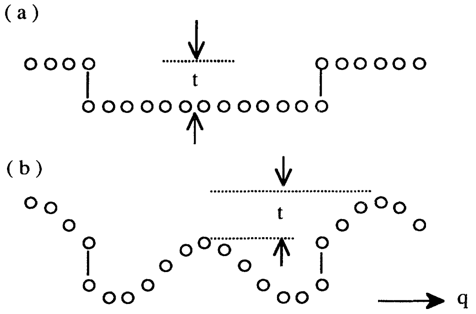

FIG. 2. (a) A rigid stepped surface with the single atomic step height t. (b) An atomic vibrational wave propagates in the stepped surface. Notice that the corresponding sinusoidal grating is shifted vertically by a step t in the neighboring terraces.

In this paper, we derive quantitatively the enhancement of thermal diffuse scattering by surface defects. It is shown that the thermal diffuse scattering manifests itself at the vicinity of the out-of-phase condition more obviously than that at the in-phase condition. In Sec. II, we outline the theoretical approach to this subject. We formulate the thermal diffuse scattering from a surface having random vacancies in Sec. III and a surface containing random steps in Sec. IV. A brief summary is given in Sec. V.

II. THEORETICAL APPROACH

The theoretical study of thermal diffuse scattering from a perfect surface had been well developed. Following Huber[6] and Mckinney, Jones, and Webb,[7] we make several assumptions, which provide us with a simple framework and an easier approach to the subject of the thermal diffuse scattering.

(i) Only the kinematic calculation is used and multiple scatterings will be ignored in this paper.

(ii) The nonpenetrating radiation is assumed so that only the scattering from the topmost surface is taken into consideration.

(iii) For simplicity, we only consider an isotropic Debye spectrum which gives a simple phonon dispersion relation

$$\omega(q)=vq \ , \tag{4}$$

where v and ω are the velocity and angular frequency of the vibrational wave, respectively.

(iv) We shall treat "classically" surface atomic vibrations. A similar result can be obtained in the quantum-mechanical scheme at higher temperatures.

In addition, we shall assume the surface defects do not significantly change the thermal vibrations in the crystal. The surface defects can affect the surface phonon modes but not the bulk modes. The major phonon relations derived from the perfect crystal, such as the representation of the normal modes, the orthogonal and completeness relations, the harmonic hamiltonian, and so on, should still hold approximately even in the presence of the surface defects. This is because the surface defects contribute a lower-dimensional (2D) disordered perturbation which is negligibly small compared to thermal vibrations in a 3D bulk crystal. Our purpose is to demonstrate the major scattering effect by surface defects. The change of the vibrations due to defect structures is a much more complicated issue. However, it should not qualitatively affect the diffuse scattering intensity derived in this paper.

The intensity of an electron beam diffracted from a surface can be written as

$$I(\mathbf{S})=|f_0|^2\sum_{m,m'}\langle\exp[i\mathbf{S}\cdot(\mathbf{r}_m-\mathbf{r}_{m'})]\rangle \ , \tag{5}$$

where f_0 is the atomic form facter and $\langle\ \rangle$ represents the thermal average. The surface atomic position is denoted by $\mathbf{r}_m=\mathbf{R}_m+\mathbf{u}_m$, where $\mathbf{R}_m$ is the position vector of a rigid lattice point and $\mathbf{u}_m$ is the corresponding atomic vibrational amplitude. Following the well-known harmonic approximation, one can write

$$\begin{aligned}\langle \exp[i\mathbf{S}\cdot(\mathbf{u}_m-\mathbf{u}_{m'})]\rangle &=\exp\{-\tfrac{1}{2}\langle[\mathbf{S}\cdot(\mathbf{u}_m-\mathbf{u}_{m'})]^2\rangle\}\\ &=e^{-2W}\exp[\langle(\mathbf{S}\cdot\mathbf{u}_m)(\mathbf{S}\cdot\mathbf{u}_{m'})\rangle]\ , \end{aligned} \tag{6}$$

where $2W=\langle(\mathbf{S}\cdot\mathbf{u}_m)^2\rangle=\langle(\mathbf{S}\cdot\mathbf{u}_{m'})^2\rangle$ is the Debye-Waller factor. After the Taylor expansion of $\exp[\langle(\mathbf{S}\cdot\mathbf{u}_m)(\mathbf{S}\cdot\mathbf{u}_{m'})\rangle]$, Eq. (5) becomes $I(\mathbf{S})=\sum_{k=0}I_k(\mathbf{S})$, where

$$I_k(\mathbf{S})=|f_0|^2e^{-2W}\sum_{m,m'}\frac{[\langle(\mathbf{S}\cdot u_m)(\mathbf{S}\cdot u_{m'})\rangle]^k}{k!}\times\exp[i\mathbf{S}\cdot(\mathbf{R}_m-\mathbf{R}_{m'})]$$

represents precisely the contribution of the k-phonon scattering process. In this paper, we only take into account the one-phonon contribution corresponding to $k=1$, and ignore all of the multiphonon scattering in which $k\geq 2$.

For the zero-phonon process $k=0$, we have

$$I_0(\mathbf{S})=|f_0|^2e^{-2W}\sum_{m,m'}\exp[i\mathbf{S}\cdot(\mathbf{R}_m-\mathbf{R}_{m'})]\ , \tag{7}$$

which is the conventional diffraction intensity including the major thermal vibrational effect at the Bragg peak; the Debye-Waller effect. Equation (7) can be rewritten as

$$I_0(\mathbf{S})=|f_0|^2e^{-2W}F(\mathbf{S})\ ,$$

where

$$F(\mathbf{S})=\sum_{m,m'}\exp[i\mathbf{S}\cdot(\mathbf{R}_m-\mathbf{R}_{m'})] \tag{8}$$

is the interference function of the rigid lattice.[7]

For the one-phonon scattering process $k=1$, we have

$$I_1(\mathbf{S})=|f_0|^2e^{-2W}\sum_{m,m'}\langle(\mathbf{S}\cdot\mathbf{u}_m)(\mathbf{S}\cdot\mathbf{u}_{m'})\rangle\times\exp[i\mathbf{S}\cdot(\mathbf{R}_m-\mathbf{R}_{m'})]\ , \tag{9}$$

which contains the major thermal scattering effect in the diffuse intensity. This is the main issue of the present work.

After expanding u_m classically as a series of normal modes of the harmonic-oscillatory waves

$$\mathbf{u}_m=\frac{1}{\sqrt{N}}\sum_{\mu,\mathbf{q}_\parallel}\mathbf{u}_{\mu,q_\parallel}\exp(-i\mathbf{q}_\parallel\cdot\mathbf{R}_m)\ ,$$

one obtains from Eq. (9)

$$I_1(\mathbf{S})=\frac{1}{N}|f_0|^2e^{-2W}\sum_{\mu,\mathbf{q}_\parallel}\langle|\mathbf{S}\cdot\mathbf{u}_{\mu,q_\parallel}|^2\rangle F(\mathbf{S}\pm\mathbf{q}_\parallel)\ , \tag{10}$$

where μ denotes an additional index labeling the various modes having the same $\mathbf{q}_\parallel$, $\mathbf{u}_{\mu,q_\parallel}$ represents the vibrational amplitude of the mode $(\mu,\mathbf{q}_\parallel)$, and N is the total number of atoms in the crystal. Equation (10) is further simpified by applying the equipartition law to the thermal energy and the Debye dispersion relation, Eq. (4). A basic formula for the one-phonon scattering intensity is then given by[7]

$$I_1(\mathbf{S})\propto\frac{t}{2\pi}\frac{a}{(2\pi)^2}|f_0|^2e^{-2W}\mathbf{S}^2\frac{k_BT}{Mv^2}\times\int dq_\perp\int d\mathbf{q}_\parallel\frac{F(\mathbf{S}\pm\mathbf{q}_\parallel)}{q_\perp{}^2+\mathbf{q}_\parallel{}^2}\ , \tag{11}$$

where $q_\perp$ is the phonon wave vector perpendicular to the surface and M is the mass of one atom. Experimentally, the ratio of the thermal diffuse intensity $I_1(\mathbf{S})$ to the peak intensity

$$I_0=I_0(\mathbf{S})\Big|_{\mathbf{S}_\parallel=\mathbf{G}_{hk}}$$

is an effective way of showing the importance of the thermal diffuse scattering because it excludes the influence of the Debye-Waller factor e^{-2W} and simply described a linear relationship with the temperature T, i.e.,

$$R=\frac{I_1(\mathbf{S})}{I_0}\propto\mathbf{S}^2k_BT\int dq_\perp\int d\mathbf{q}_\parallel\frac{F(\mathbf{S}\pm\mathbf{q}_\parallel)}{q_\perp{}^2+\mathbf{q}_\parallel{}^2}\ . \tag{12}$$

Equations (10) and (11) were applied to the perfect surfaces in the previous studies.[6,7] It is a very important feature in these two equations that the one-phonon scattering intensity contains the interference function $F(\mathbf{S}\pm\mathbf{q}_\parallel)$, which mainly depends on the rigid surface morphology. This allows us to extend the study to imperfect surfaces which can have various forms of the interference function. It will be shown in the following that a significant difference of the thermal diffuse scattering exists between a perfect surface and an imperfect one.

A. Thermal diffuse scattering from a defect-free surface

For a perfect surface, the interference function is given by a sum of δ functions which are located at the 2D Bragg positions $\mathbf{G}_{hk}$, i.e.,

$$F(\mathbf{S})=\left[\frac{2\pi}{a}\right]^2\sum_{h,k}\delta(\mathbf{S}_\parallel-\mathbf{G}_{hk})\ .$$

Correspondingly, Eq. (11) becomes

$$I_1(\mathbf{S})\propto\frac{t}{2\pi}|f_0|^2e^{-2W}\mathbf{S}^2\frac{k_BT}{Mv^2}\times\int dq_\perp\int d\mathbf{q}_\parallel\frac{\sum\delta(\mathbf{S}_\parallel-G_{hk}\pm\mathbf{q}_\parallel)}{q_\perp{}^2+\mathbf{q}_\parallel{}^2}\ . \tag{13}$$

The δ functions in Eq. (13) show that only those vibrational modes satisfying $\mathbf{S}_\parallel-\mathbf{G}_{hk}\pm\mathbf{q}_\parallel=\mathbf{0}$, i.e., obeying the momentum conservation law, can contribute to the diffuse intensity at the 2D reciprocal space position $\mathbf{S}_\parallel$, as shown in Fig. 3. This is the basis of the statement that the thermal diffuse scattering from a perfect surface is due to the vibrational wave-grating diffraction, as demonstrated in the introduction. The calculation of Eq. (13) can be carried out easily,[6,7] which gives Eq. (1), the conventional one-phonon thermal diffuse intensity.

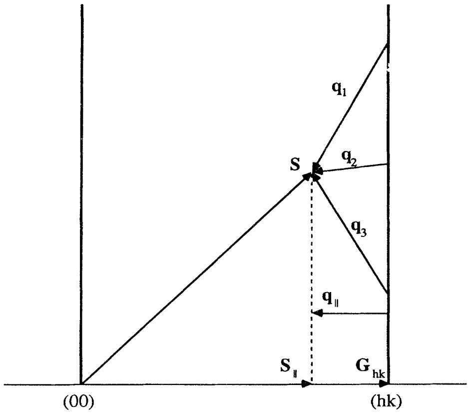

FIG. 3. A vector diagram in the 2D reciprocal space shows the one-phonon scattering from a defect-free-surface. Only those phonon modes such as $\mathbf{q}_1$, $\mathbf{q}_2$, and $\mathbf{q}_3$, which obey the momentum conservation law $\mathbf{S}_\parallel - \mathbf{G}_{hk} = \pm\mathbf{q}_\parallel$, can contribute to the diffuse intensity of the electron beam at the 2D position $\mathbf{S}_\parallel$, where $\mathbf{G}_{hk}$ are the 2D Bragg vectors.

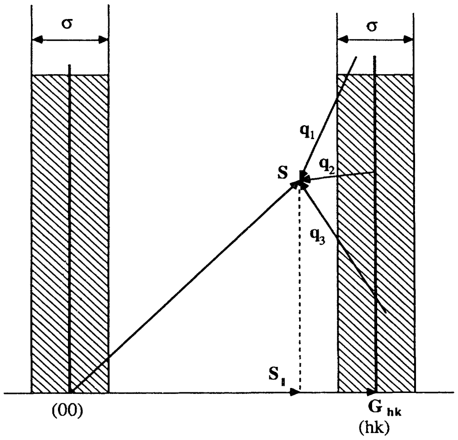

FIG. 4. A vector diagram shows the one-phonon scattering from an imperfect surface which has broadened the Bragg rods in the 2D reciprocal space. All of those phonon modes, such as $\mathbf{q}_1$, $\mathbf{q}_2$, and $\mathbf{q}_3$, which project onto the inside of the Bragg rods of a diameter σ, $|\mathbf{S}_\parallel - \mathbf{G}_{hk} \pm \mathbf{q}_\parallel| \le \sigma$, can contribute to the diffuse intensity at $\mathbf{S}_\parallel$.

B. Thermal diffuse scattering from imperfect surfaces

For imperfect surfaces, the interference function $F(\mathbf{S})$ is very often represented by a series of broadened Bragg rods in the 2D reciprocal space. If the δ functions in Eq. (13) are replaced to represent the broadened rods, the wave-grating diffraction law, Eq. (3), will no longer be applicable. As shown in Fig. 4, all of those vibrational modes which project onto the vicinity of the broadened Bragg rods, i.e., satisfying

$$|\mathbf{S}_\parallel - \mathbf{G}_{hk} \pm \mathbf{q}_\parallel| \le \sigma \ , \tag{14}$$

can contribute to the diffuse intensity at the position $\mathbf{S}_\parallel$, where σ represents the size of the cross section of the Bradd rods and is determined by the corresponding peak width. Only when $\sigma = 0$, can Eq. (3) be held.

The deviation from the simple conservation law of Eq. (3) will in general lead to the increase of the thermal diffuse intensity. As shown in Eq. (10), each phonon mode contributes a scattering intensity proportional to $\langle (\mathbf{u}_{\mu,q_\parallel})^2 \rangle$. According to the equipartition law of the thermal energy and Eq. (4), $\langle (\mathbf{u}_{\mu,q_\parallel})^2 \rangle \propto q^{-2}$, where $q^2 = q_\perp{}^2 + \mathbf{q}_\parallel{}^2$. Therefore those modes with smaller q, i.e., the long-wavelength phonons, make a larger contribution to the total diffuse intensity. For the defect-free surface, the conservation law forbids any modes with q smaller than $|\mathbf{S}_\parallel - \mathbf{G}_{hk}|$ since

$$\mathbf{q}^2 = q_\perp{}^2 + \mathbf{q}_\parallel{}^2 \ge \mathbf{q}_\parallel{}^2 = |\mathbf{S}_\parallel - \mathbf{G}_{hk}|^2 \ .$$

However, for an imperfect surface, this restriction is lifted because Eq. (3) no longer holds. Instead, Eq. (14) gives

$$q \ge |\mathbf{q}_\parallel| \ge |\mathbf{S}_\parallel - \mathbf{G}_{hk}| - \sigma \ , \tag{15}$$

where $|\mathbf{S}_\parallel - \mathbf{G}_{hk}| > \sigma$ because the diffuse intensity is measured at the reciprocal-space position far away from the Bragg peak. Therefore all those phonon modes of smaller q, which are forbidden in a perfect surface but satisfy Eq. (15), are allowed to contribute to the diffuse scattering. The diffuse intensity must be enhanced by these long-wavelength phonons.

The above interpretation qualitatively reveals the physical origin of the enhancement of the thermal scattering by surface defects. The quantitative feature of this effect should depend on the detail structure of the surface defects. As one of the simple examples, let us consider a surface having finite-size domains. Given the "Warren approximation" for the domains,[24] one expresses the interference function of the surface as[25]

$$F(\mathbf{S}) = \sum_{m,m'} \exp[i\mathbf{S}\cdot(\mathbf{R}_m - \mathbf{R}_{m'})] \approx \left[\frac{L}{a}\right]^2 \exp\left[-\frac{(\mathbf{S}_\parallel - \mathbf{G}_{hk})^2}{\sigma^2}\right] , \tag{16}$$

where L is the average domain size and $\sigma = 2\pi/L$ is the Gaussian width proportional to the size of the broadened Bragg rods. Inserting Eq. (16) into Eq. (11), we obtain the diffuse intensity

$$I_1(\mathbf{S}) \propto |f_0|^2 e^{-2W} \mathbf{S}^2 \frac{k_B T}{M v^2} \times \int dq_\perp \int d\mathbf{q}_\parallel \frac{\exp[-(\mathbf{S}_\parallel - \mathbf{G}_{hk} \pm \mathbf{q}_\parallel)^2/\sigma^2]}{q_\perp{}^2 + \mathbf{q}_\parallel{}^2} ,$$

where the integral has a closed-form solution which is proportional to the Kummer function, i.e.,

$$\int dq_\perp \int d\mathbf{q}_\parallel \frac{\exp[-(\mathbf{S}_\parallel - \mathbf{G}_{hk} \pm \mathbf{q}_\parallel)^2/\sigma^2]}{q_\perp{}^2 + \mathbf{q}_\parallel{}^2} \propto \sigma\phi(\tfrac{1}{2};1;-|\mathbf{S}_\parallel - \mathbf{G}_{hk}|^2/\sigma^2) \ .$$

The Kummer function ϕ is defined as[26]

$$\phi(\alpha;\beta;z) = \sum_{m=0} \frac{\Gamma(\alpha+m)\Gamma(\beta)}{\Gamma(\alpha)\Gamma(\beta+m)} \frac{z^m}{m!} \ ,$$

where $\Gamma(x)$ is the gamma function. As is well known,[26] the Kummer function has an asymptotic form at large q: $\phi(1-\alpha/2;1;-q^2/\sigma^2) \sim (\sigma/q)^\alpha$. Thus the ratio of the thermal diffuse intensity to the peak intensity is given by

$$R = \frac{I_1(\mathbf{S})}{I_0} \propto \frac{\sigma^2 \mathbf{S}^2 k_B T}{|\mathbf{S}_\parallel - \mathbf{G}_{hk}|} \ . \tag{17}$$

Equation (17) shows quantitatively the enhanced thermal diffuse scattering by the finite-size effect, where the ratio R is linearly proportional to σ^2 with $\sigma = 2\pi/L$. The smaller the surface domain size L, the stronger the thermal diffuse scattering effect. Similar conclusion can be drawn for a finite 2D harmonic lattice,[25] where $R \propto \sigma^2 |\mathbf{S}_\parallel - \mathbf{G}_{hk}|^{-2+\eta}$. More importantly, Eq. (17) indicates that the enhancement of the thermal diffuse scattering is basically due to the broadening of the interference function (Bragg peaks), which agrees with our previous qualitative interpretation. This broadening could be caused by many different kinds of surface defects. In Secs. III and IV, we will show quantitatively how point defects and surface steps can affect the thermal diffuse intensity.

III. THERMAL DIFFUSE SCATTERING FROM A SURFACE CONTAINING RANDOMLY DISTRIBUTED VACANCIES

For a surface with the top layer containing randomly distributed vacancies, Pimbly and Lu have given an exact solution for the interference function:[16]

$$F(\mathbf{S}) = [1 + f^2 - 2f\cos(S_\perp t - \eta)]n(1-n) + \left[\frac{2\pi}{a}\right]^2 [(1-n)^2 + n^2 f^2 + 2n(1-n)f\cos(S_\perp t - \eta)] \times \delta(\mathbf{S}_\parallel - \mathbf{G}_{hk}) \ , \tag{18}$$

where n is the vacancy concentration in the top layer and $fe^{i\eta}$ is the relative atomic form factor between the first and the second layer atoms. Equation (18) was originally applied to the diffraction from a 2D adsorbed overlayer with AAA stacking, where the adsorbed atoms can be different from the substrate atoms. For the clean surface we are interested in, i.e., a surface having vacancies, the atoms in the first and second layer are identical.

A. Surface with *AAA* stacking

For the AAA stacking surface where $f = 1$, $\eta = 0$, Eq. (18) becomes

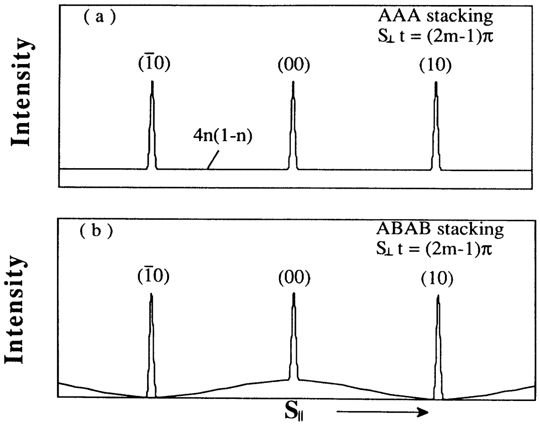

FIG. 5. (a) The angular profiles of the electron beams diffracted from an AAA stacking surface with randomly distributed vacancies, where $S_\perp t = (2m-1)\pi$, corresponding to the out-of-phase diffraction conditions. Notice the substantial constant background throughout the entire Brillouin zones. (b) The angular profiles from an $ABAB$ stacking surface with randomly distributed vacancies. Here $S_\perp t = (2m-1)\pi$, which are the out-of-phase conditions for the (00) beam, but are the in-phase conditions for the (10) or (10) beams. This gives a background intensity which is not constant but is slowly varying throughout the entire Brillouin zones.

$$F(\mathbf{S}) = 2n(1-n)[1-\cos(S_\perp t)] + \left[\frac{2\pi}{a}\right]^2 \{1 - 2n(1-n)[1-\cos(S_\perp t)]\} \times \delta(\mathbf{S}_\parallel - \mathbf{G}_{hk}) \ , \tag{19}$$

which is a δ function superimposed on a constant background. At the in-phase condition $S_\perp t = 2m\pi$, the background vanishes. At the out-of-phase condition $S_\perp t = (2m-1)\pi$, the background has a maximum value $4n(1-n)$, as shown in Fig. 5(a).

The calculation of the thermal diffuse intensity is carried out in the following. The δ-function term in Eq. (19) is inserted into Eq. (11), which turns out to be the conventional thermal diffuse intensity $I_1'(\mathbf{S})$ as is given by Eq. (1). However, by inserting the background term in Eq. (19) into Eq. (10), which is equivalent to Eq. (11), we then obtain an additional constant intensity

$$|f_0|^2 e^{-2W} \{2n(1-n)[1-\cos(S_\perp t)] \langle (\mathbf{S}\cdot\mathbf{u}_m)^2 \rangle \} \ .$$

Here, we have used the identity

$$\frac{2}{N} \sum_{\mu,\mathbf{q}_\parallel} \langle |\mathbf{S}\cdot\mathbf{u}_{\mu,q_\parallel}|^2 \rangle = \langle (\mathbf{S}\cdot\mathbf{u}_m)^2 \rangle \ .$$

Thus the one-phonon scattering intensity for the (00) beam is given by

$$I_1(\mathbf{S}) = I_1'(\mathbf{S}) + |f_0|^2 e^{-2W} \{2n(1-n)[1-\cos(S_\perp t)] \times \langle (S_\perp u_\perp)^2 \rangle \} \ .$$

$I_1'(\mathbf{S})$ can manifest itself at the in-phase condition, where the constant background intensity vanishes. Note that the factor $\langle (S_\perp u_\perp)^2 \rangle$ is just the Debye-Waller factor $2W$. Combined with the background intensity in Eq. (19), the ratio of the total background intensity to peak intensity is given by

$$R \propto \begin{cases} R' \quad \text{for the in-phase condition} \\ R' + 2n(1-n)[1-\cos(S_\perp t)](1+\langle (S_\perp u_\perp)^2 \rangle) \\ \qquad\qquad \text{for the out-of-phase condition ,} \end{cases} \tag{20}$$

where R' is the conventional one-phonon contribution

$$R' \propto \frac{\mathbf{S}^2 k_B T}{|\mathbf{S}_\parallel|} \; . \tag{21}$$

It is concluded that due to the thermal diffuse scattering, the background intensity can be increased by a factor of $1+\langle (S_\perp u_\perp)^2 \rangle$ at other than in-phase conditions. The value of $\langle (S_\perp u_\perp)^2 \rangle$ can range from 1 to 10 $[\sqrt{\langle u_\perp{}^2 \rangle} \sim 0.05t$ to $0.10t$, and $S_\perp t \sim 2\pi$ to $10\pi]$. Since $\langle (S_\perp u_\perp)^2 \rangle = 2W \propto T$, this effect may be observable at a reasonably high temperature. However, this enhancement can only occur when the surface contains vacancies. If the vacancy concentration $n=0$, the background terms due to vacancies, as shown in Eqs. (19) and (20), will vanish.

B. Surface with *ABAB* stacking

For *ABAB* stacking surface, as shown in Figs. 6(a) and 6(b), the first-layer atoms are displaced laterally along the $\mathbf{a}+\mathbf{b}$ (or $\mathbf{a}-\mathbf{b}$) direction with respect to the second layer. Here $\mathbf{a}=a\mathbf{i}$ and $\mathbf{b}=a\mathbf{j}$ are two orthogonal unit vectors of a square unit mesh. Therefore Eq. (18) cannot be directly applied to the case of *ABAB* stacking.

Consider a one-dimensional model. As shown in Fig. 6(c), if we choose a unit cell consisting of *A*-*B* biatoms, an *ABAB* stacking can be transformed into a quasi-*AAA* stacking, where the first layer has a different form factor from that in the second layer. Under this model (along the $\mathbf{a}+\mathbf{b}$ direction), Eq. (18) can still be used approximately for the *ABAB* stacking surface in which the relative form factor $fe^{i\eta} \neq 1$.

The unit cells in the first and the second layer are chosen according to Fig. 6(c). The form factor relative to the center of the unit cell is given by

$$f_1 = f_0 \varepsilon \exp\left[i \left[-\frac{S_\perp t}{2} - \frac{\mathbf{S}_\parallel \cdot (\mathbf{a}+\mathbf{b})}{4} \right] \right] + f_0 \exp\left[i \left[\frac{S_\perp t}{2} + \frac{\mathbf{S}_\parallel \cdot (\mathbf{a}+\mathbf{b})}{4} \right] \right] \quad \text{for the first layer}$$

$$f_2 = f_0 \exp\left[i \left[\frac{S_\perp t}{2} - \frac{\mathbf{S}_\parallel \cdot (\mathbf{a}+\mathbf{b})}{4} \right] \right] + f_0 \varepsilon \exp\left[i \left[-\frac{S_\perp t}{2} + \frac{\mathbf{S}_\parallel \cdot (\mathbf{a}+\mathbf{b})}{4} \right] \right] \quad \text{for the second layer .}$$

The penetration factor ε (which is necessary when we calculate the relative scattering amplitude of the atoms inside a unit cell), can be expressed as

$$\varepsilon = \exp\left[-\frac{t}{\lambda_c} \right] , \tag{22}$$

where λ_c is the mean free path of the electron beam and is energy dependent.

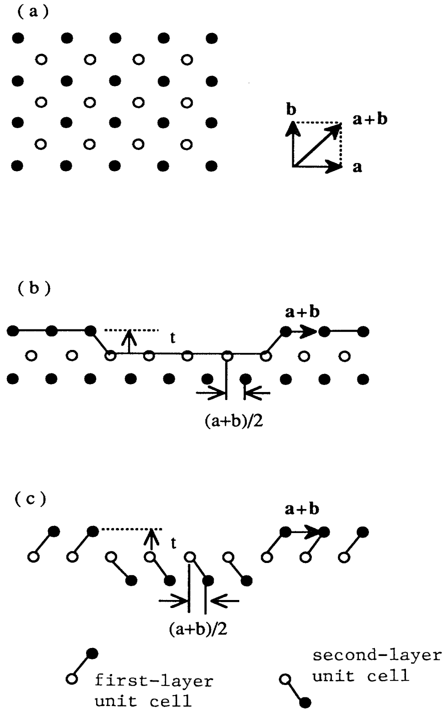

FIG. 6. (a) A top view of an *ABAB* stacking surface with a square unit mesh, where $\mathbf{a}=a\mathbf{i}$ and $\mathbf{b}=a\mathbf{j}$ are two orthogonal unit vectors. The solid dots and the open circles are the *A* atoms (in the first layer) and the *B* atoms (in the second layer), respectively. (b) The side view of the *ABAB* stacking surface along the $\mathbf{a}+\mathbf{b}$ direction. The figure demonstrates the atomic steps with a single step height t. (a) and (b) show that the *A* atoms in the first layer are displaced laterally with respect to the *B* atoms in the second layer by a vector $(\mathbf{a}+\mathbf{b})/2$. (c) If the biatom *A*-*B* is chosen as a basis, the surface could be treated as a quasi-*AAA* stacking surface where the *A*-*B* biatoms in the first layer are displaced laterally with respect to the *A*-*B* biatoms in the second layer by a vector of $\mathbf{a}+\mathbf{b}$ which corresponds to the lattice spacing in this direction. Note that the *A*-*B* biatoms in the first layer have a different orientation from those in the second layer, which will give a different scattering form factor.

The relative form factor is then given by $fe^{i\eta}=f_1/f_2$. Accordingly, the interference function for surfaces with *ABAB* stacking can be obtained from Eq. (18), which is

$$F(\mathbf{S}_\parallel)=2n(1-n)(1-\varepsilon)^2\left[1-\cos\left[\frac{\mathbf{S}_\parallel\cdot(\mathbf{a}+\mathbf{b})}{2}\right]\right]+\left[\frac{2\pi}{a}\right]^2(1+\varepsilon)^2\delta(\mathbf{S}_\parallel-\mathbf{G}_{hk}) \tag{23a}$$

at $S_\perp t=2m\pi$ and

$$F(\mathbf{S}_\parallel)=2n(1-n)(1-\varepsilon)^2\left[1+\cos\left[\frac{\mathbf{S}_\parallel\cdot(\mathbf{a}+\mathbf{b})}{2}\right]\right]+\left[\frac{2\pi}{a}\right]^2(1-\varepsilon)^2\delta(\mathbf{S}_\parallel-\mathbf{G}_{hk}) \tag{23b}$$

at $S_\perp t=(2m-1)\pi$.

As shown in Fig. 5(b), the background intensity for *ABAB* stacking is not a constant but slowly varies throughout the Brillouin zone, which is different from that for the *AAA* stacking surface shown in Fig. 5(a). Recently, Kang *et al.*[27] have proposed a random layer-by-layer epitaxy model on fcc (100) substrates, which exhibits a similar behavior as that shown in Fig. 5(b). Although this model is more rigorous for the case of 2D *ABAB* stacking, it does not provide a closed form for the interference function when the penetration factor ε is included. Therefore, for the present purpose, we still use Eq. (23).

By inserting Eqs. (23a) and (23b) into either Eq. (10) or (11), we obtain the thermal diffuse intensity for the specular beam,

$$I_1(\mathbf{S})=I_1'(\mathbf{S})+|f_0|^2e^{-2W}2n(1-n)(1-\varepsilon)^2\times\left[1-A\cos\left[\frac{\mathbf{S}_\parallel\cdot(\mathbf{a}+\mathbf{b})}{2}\right]\right]S_\perp{}^2\langle u_\perp^2\rangle$$

for the in-phase conditions and

$$I_1(\mathbf{S})=I_1'(\mathbf{S})+|f_0|^2e^{-2W}2n(1-n)(1-\varepsilon)^2\times\left[1+A\cos\left[\frac{\mathbf{S}_\parallel\cdot(\mathbf{a}+\mathbf{b})}{2}\right]\right]S_\perp{}^2\langle u_\perp^2\rangle$$

for the out-of-phase conditions. A is a constant given by

$$A=\int dq_\perp\int d\mathbf{q}_\parallel\frac{\dfrac{\cos[\mathbf{q}_\parallel\cdot(\mathbf{a}+\mathbf{b})/2]}{q_\perp^2+\mathbf{q}_\parallel^2}}{\displaystyle\int dq_\perp\int d\mathbf{q}_\parallel\frac{1}{q_\perp^2+\mathbf{q}_\parallel^2}}\,,$$

which is estimated to be ~0.6. Experimentally, $S_\parallel \ll 2\pi/a$ so that $\cos[\mathbf{S}_\parallel\cdot(\mathbf{a}+\mathbf{b})/2]\approx 1$, i.e., the slow change of the background intensity is negligible. Thus the ratio of the background intensity to peak intensity is

$$R\propto\begin{cases}R'+\Omega[(2n-1)^{-2}-1]S_\perp{}^2\langle u_\perp{}^2\rangle & \text{for the in-phase condition}\\ R'+[(2n-1)^2-1](1+BS_\perp{}^2\langle u_\perp{}^2\rangle) & \text{for the out-of-phase condition}\,,\end{cases} \tag{24}$$

where R' is again the conventional one-phonon scattering contribution given by Eq. (21). The constants are given by

$$\Omega=\frac{1-A}{2}\left[\frac{1-\varepsilon}{1+\varepsilon}\right]^2$$

and $B=(1+A)/2\sim 0.8$. Usually, $\Omega \ll 1$. For instance, in the Pb(100) surface, $\Omega\approx 0.004$ (the mean free path $\lambda_c\sim 10$ Å at $E\sim 30$ eV and the single-step height $t=2.45$ Å). Therefore, at the in-phase condition the constant background term in the ratio is practically very small compared to that at the out-of-phase condition. Besides, the constant B can differ from what we have estimated from the Debye spectrum. It can be varied due to the contributions from other phonon modes, expecially the surface phonon modes. This would give a somewhat larger value of B. Practically, B is in the range of $0.8<B<1$ and can only be determined by experiment.

As a conclusion, Eq. (24), which describes the *ABAB* stacking surface, is practically identical to Eq. (20) describing the *AAA* stacking surface.

IV. THERMAL DIFFUSE SCATTERING FROM A SURFACE WITH MULTILAYER OF STEPS

As an electron beam is diffracted from a surface containing multilayers of randomly distributed steps, the angular profile can be described approximately by a Lorentzian function:[28,29]

$$F(\mathbf{S})=\frac{1}{1+\left[\dfrac{|\mathbf{S}_\parallel-\mathbf{G}_{hk}|}{\sigma_L}\right]^2}\,, \tag{25}$$

where the Lorentzian width σ_L is a periodic oscillation function of $S_\perp t$. σ_L reaches a maximum at the out-of-phase condition and equals zero at the in-phase condition. Correspondingly, the thermal diffuse intensity for the (00) beam is given by

$$I_1(\mathbf{S})\propto|f_0|^2e^{-2W}\mathbf{S}^2k_BT\times\int dq_\perp\int d\mathbf{q}_\parallel\frac{1}{\left[1+\left[\dfrac{|\mathbf{S}_\parallel-\mathbf{G}_{hk}|}{\sigma_L}\right]^2\right](q_\perp{}^2+\mathbf{q}_\parallel{}^2)}\,. \tag{26}$$

The integral in Eq. (26) has an asymptotic form at large $|\mathbf{S}_\parallel-\mathbf{G}_{hk}|$:

$$\int dq_\perp\int d\mathbf{q}_\parallel\frac{1}{\left[1+\left[\dfrac{|\mathbf{S}_\parallel-\mathbf{G}_{hk}|}{\sigma_L}\right]^2\right](q_\perp{}^2+\mathbf{q}_\parallel{}^2)}\propto\frac{\sigma_L{}^2}{|\mathbf{S}_\parallel-\mathbf{G}_{hk}|}\ln\left[\frac{4|\mathbf{S}_\parallel-\mathbf{G}_{hk}|}{\sigma_L}\right].$$

The thermal diffuse intensity, Eq. (26), then becomes

$$I_1(\mathbf{S})\propto|f_0|^2e^{-2W}\mathbf{S}^2k_BT\frac{\sigma_L{}^2}{|\mathbf{S}_\parallel-\mathbf{G}_{hk}|}\ln\left[\frac{4|\mathbf{S}_\parallel-\mathbf{G}_{hk}|}{\sigma_L}\right]. \tag{27}$$

The ratio of I_1 to I_0 reduces to

$$R \propto \mathbf{S}^2 k_B T \frac{\sigma_L{}^2}{|\mathbf{S}_\parallel - \mathbf{G}_{hk}|} \ln \left[\frac{4|\mathbf{S}_\parallel - \mathbf{G}_{hk}|}{\sigma_L} \right] . \tag{28}$$

The Lorentzian line shape produces a thermal diffuse intensity which has a wing structure $\sim |\mathbf{S}_\parallel - \mathbf{G}_{hk}|^{-1} \ln(4|\mathbf{S}_\parallel - \mathbf{G}_{hk}|/\sigma_L)$. This is different from Eqs. (1) and (17), where the wing structure has a form of $|\mathbf{S}_\parallel - \mathbf{G}_{hk}|^{-1}$. On the other hand, Eq. (27) shows that for the Lorentzian type of interference function, the thermal diffuse intensity is proportional to the square of Lorentzian width $\sigma_L{}^2$. This is similar to Eq. (17) even though the interference function is different. The rougher the surface, the broader the beam profile and the stronger the thermal diffuse intensity. More importantly, the Lorentzian width σ_L is a periodic oscillation function of $S_\perp t$, which gives the strongest thermal diffuse intensity as $S_\perp t$ approaches $(2m-1)\pi$, i.e., the out-of-phase conditions. On the contrary, at the in-phase conditions, R is very small and depends only on the instrumental response. For instance, if the Lorentzian line shape at the out-of-phase condition has a peak width which is about 10 times broader than that at the in-phase condition, the corresponding thermal diffuse intensity should be at least 100 higher than that at the in-phase condition.

V. SUMMARY

The effect of surface defects on thermal diffuse scattering has been studied from the viewpoint of a LEED experiment in this paper. It is concluded that the surface defects, such as vacancies, adatoms, and steps, can increase the thermal diffuse intensity under non-in-phase conditions. This effect is basically caused by the surface imperfections which break up the periodic crystal ordering and lead to a deviation of the momentum conservation law. Recently, a phase containing a high density of vacancies has been observed[30] in the Pb(100) surface at an elevated temperature. The energy-dependent background intensities were measured at out-of-phase diffraction conditions using the high-resolution low-energy electron diffraction technique. These measured data have been described very well by the equations derived in Sec. III and therefore are consistent with our predictions.

ACKNOWLEDGMENTS

We thank Professor G. -C. Wang for a critical reading of the manuscript. This work was supported by the National Science Foundation under Grant No. 8906003.

---

[1] D. L. Mills and S. Y. Tong, in *Chemistry and Physics of Solid Surfaces IV,* edited by R. Vanselow and R. Howe (Springer-Verlag, Berlin, 1982), p. 341.

[2] H. Ibach and D. L. Mills, *Electron Energy Loss Spectroscopy* (Academic, New York, 1982).

[3] V. Celli, D. Himes, V. Bortolani, G. Santoro, J. P. Toennies, and G. Zhang, Surf. Sci. **242**, 518 (1991).

[4] V. Celli, D. Himes, P. Tran, J. P. Toennies, Ch. Wöll, and G. Zhang, Phys. Rev. Lett. **66**, 3160 (1991).

[5] R. F. Wallis and A. A. Maradudin, Phys. Rev. **148**, 962 (1966).

[6] D. L. Huber, Phys. Rev. **153**, 772 (1966).

[7] J. T. Mckinney, E. R. Jones, and M. B. Webb, Phys. Rev. **160**, 523 (1967).

[8] R. F. Barnes, M. G. Lagally, and M. B. Webb, Phys. Rev. **171**, 627 (1968).

[9] H. Ibach and S. Lehwald, Surf. Sci. **176**, 629 (1986).

[10] P. L. De Andres, P. J. Rous, and J. B. Pendry, Surf. Sci. **193**, 1 (1988).

[11] G. S. Blackman, M. -L. Xu, D. F. Ogletree, M. A. Van Hove, and G. A. Somorjai, Phys. Rev. Lett. **61**, 2352 (1988).

[12] M. Henzler, in *Electron Spectroscopy for Surface Analysis,* edited by H. Ibach (Springer-Verlag, Berlin, 1977), p. 117.

[13] M. G. Lagally, in *Chemistry and Physics of Solid Surfaces IV* (Ref. 1), p. 281.

[14] P. J. Rous and J. B. Pendry, Surf. Sci. **173**, 1 (1986).

[15] P. J. Rous and J. B. Pendry, Surf. Sci. **155**, 241 (1985).

[16] J. M. Pimbley and T. -M. Lu, Surf, Sci. **139**, 360 (1984).

[17] K. Heinz, D. K. Saldin, and J. B. Pendry, Phys. Rev. Lett. **55**, 2312 (1985).

[18] P. J. Rous, J. B. Pendry, D. K. Saldin, K. Heinz, K. Müller, and N. Bickel, Phys. Rev. Lett. **57**, 2951 (1986).

[19] K. Heinz, K. Müller, W. Popp, and H. Lindner, Surf. Sci. **173**, 366 (1986).

[20] J. B. Pendry and D. K. Saldin, Surf. Sci. **145**, 33 (1984).

[21] D. K. Saldin, J. B. Pendry, M. A. Van Hove, and G. A. Somorjai, Phys. Rev. B **31**, 1216 (1985).

[22] E. R. Jones, J. T. Mckinney, and M. B. Webb, Bull. Am. Phys. Soc. **10**, 324 (1965).

[23] J. Aldag and R. M. Stern, Phys. Rev. Lett. **14**, 857 (1965).

[24] B. E. Warren, Phys. Rev. **59**, 693 (1941).

[25] P. Dutta and S. K. Sinha, Phys. Rev. Lett. **47**, 50 (1981).

[26] *Handbook of Mathematical Functions,* edited by M. Abramowitz and I. A. Stegun (Dover, New York, 1970).

[27] H. C. Kang, D. K. Flynn-Sanders, P. A. Thiel, and J. W. Evans, Surf. Sci. **256**, 205 (1991).

[28] T. -M. Lu and M. G. Lagally, Surf. Sci. **120**, 47 (1982).

[29] H. -N. Yang, T. -M. Lu, and G. -C. Wang. Phys. Rev. B **43**, 4717 (1991).

[30] H. -N. Yang, K. Fang, G. -C. Wang, and T. -M. Lu, Phys. Rev. B **44**, 1306 (1991).